

Decay property of the $X(3842)$ as the $\psi_3(1^3D_3)$ state

Wei Li,^{1,2,3,*} Su-Yan Pei,^{1,2,3} Tianhong Wang,⁴ Tai-Fu Feng,^{1,2,3} and Guo-Li Wang^{1,2,3,†}

¹Department of Physics, Hebei University, Baoding 071002, China

²Hebei Key Laboratory of High-Precision Computation
and Application of Quantum Field Theory, Baoding 071002, China

³Hebei Research Center of the Basic Discipline for Computational Physics, Baoding 071002, China

⁴School of Physics, Harbin Institute of Technology, Harbin 150001, China



(Received 19 September 2023; accepted 9 January 2024; published 12 February 2024)

In this paper, the new particle $X(3842)$ discovered by the LHCb Collaboration is identified to be the $\psi_3(1^3D_3)$ state. We study its strong decays with the combination of the Bethe-Salpeter method and the 3P_0 model. Its electromagnetic (EM) decay is also calculated by the Bethe-Salpeter method within the Mandelstam formalism. The strong decay widths are $\Gamma[X(3842) \rightarrow D^0 \bar{D}^0] = 1.27$ MeV and $\Gamma[X(3823) \rightarrow D^+ D^-] = 1.08$ MeV, and the ratio is $\mathcal{B}[X(3842) \rightarrow D^+ D^-]/\mathcal{B}[X(3823) \rightarrow D^0 \bar{D}^0] = 0.84$. The EM decay width is $\Gamma[X(3842) \rightarrow \chi_{c2} \gamma] = 0.29$ MeV. We also estimate the total width to be 2.87 MeV, which is in good agreement with the experimental data $2.79^{+0.86}_{-0.86}$ MeV. Since the used relativistic wave functions include different partial waves, we also study the contributions of different partial waves in electromagnetic decay.

DOI: 10.1103/PhysRevD.109.036011

I. INTRODUCTION

It is a known fact that spectra of charm mesons have been experimentally mapped with great precision since the discovery of the J/ψ resonance [1,2]. Theoretically, the potential models [3] can well describe the spectra and properties of these states. Charmonium, a bound state composed of charm and anticharm quarks that is useful for testing the validity of phenomenological models, such as the quark potential model [4], and which has foreseen rich and meaningful quarkonium spectra, plays an important role in quantum chromodynamics (QCD). In recent decades, Belle, BABAR, and BESIII Collaborations have observed many new charmoniumlike states, commonly known as the XYZ states [5], such as $X(3872)$ [6], $X(3930)$ [7,8], $X(3940)$ [9,10], $X(3915)$ [11], $X(3860)$ [12], etc. Some of them are traditional excited charmonia, others are considered to be exotic in nature. Interest in charmonium spectroscopy was renewed as more of these states were discovered.

Recently, the LHCb Collaboration discovered a new narrow, but very high statistical significance, resonance state, named $X(3842)$, in the decay modes $X(3842) \rightarrow$

$D^0 \bar{D}^0$ and $X(3842) \rightarrow D^+ D^-$ [13]. The mass and width of this state are measured to be

$$M_{X(3842)} = 3842.71 \pm 0.16 \pm 0.12 \text{ MeV},$$

$$\Gamma_{X(3842)} = 2.79 \pm 0.51 \pm 0.35 \text{ MeV},$$

where the first uncertainty is statistical and the second is systematic. Based on observed mass and narrow natural width, this new state can be interpreted as the unobserved $\psi_3(1^3D_3)$ charmonium state with $J^{PC} = 3^{--}$. The BESIII Collaboration confirmed this particle in the process $e^+ e^- \rightarrow \pi^+ \pi^- X(3842) \rightarrow \pi^+ \pi^- D^+ D^-$, and evidence with a significance of 4.2σ was found [14].

At present, the experimental data of $X(3842)$ are relatively sparse. However, theory had predicted the $\psi_3(1^3D_3)$ state to have a natural width 0.5–4 MeV [15–17] and mass in the range 3806–3912 MeV [4,18–24]. These studies show that its dominate decay channel is decay to $D^+ D^-$ and $D^0 \bar{D}^0$. In addition, the radiative decay of $X(3842)$ decay to $\chi_{c2} \gamma$ is not negligible [17]. As is well known, these open-flavor strong decays closely relate to the nonperturbative properties, and our knowledge is rather poor in this region. A complete understanding of the QCD vacuum is necessary to fully solve this problem. Although we can expect lattice QCD calculation to provide us with more reliable theoretical predictions in the future, for now, we still need to build phenomenological models to study properties of this kind of decay, e.g., the 3P_0 model [25–27], the flux-tube mode [28], the Cornell model [3,29] with a vector confinement

*Corresponding author: watliwei@163.com

†Corresponding author: wgl@hbu.edu.cn

Published by the American Physical Society under the terms of the Creative Commons Attribution 4.0 International license. Further distribution of this work must maintain attribution to the author(s) and the published article's title, journal citation, and DOI. Funded by SCOAP³.

interaction, the model in Ref. [30] with a scalar confinement interaction, and the field correlator method [31].

In previous studies [32,33], we found that the relativistic effect of a highly excited state is very large; we need to choose the relativistic method to calculate. The Salpeter equation [34], which is the instantaneous version of the Bathe-Salpeter (BS) equation [35], is suitable for the heavy meson, especially the double-heavy meson. We have solved the complete Salpeter equations for different states; see Refs. [36–39] or the summary papers [40,41]. We have also improved this method to calculate the transition amplitude [42] with the relativistic wave function as input. Using this improved BS method, we can get relatively accurate theoretical results, which are in good agreement with the experimental data, see Refs. [43–45] for examples. The 3P_0 model (quark pair creation model) is a nonrelativistic model. This model is widely used in the Okubo-Zweig-Iizuka allowed strong decays of a meson [17,30,46]. In Refs. [47–49], the 3P_0 model is extended to the relativistic case, where the input relativistic wave functions come from the strict solution of the Salpeter equation. So in this paper, the strong decay of $X(3842)$ as the $\psi_3(1^3D_3)$ state is studied by the combination of the Salpeter equation and the 3P_0 model, and its main electromagnetic (EM) decay is also studied by the improved BS method. In addition, since the relativistic wave function contains different partial waves [41], we also study the contributions of different partial waves in EM decay.

The paper is organized as follows. In Sec. II, we show the relativistic wave functions of initial and final mesons. The formula to calculate the strong and EM decay of $X(3842)$ is also present in this section. In Sec. III, we give the results and make comparisons with other theoretical predictions and experimental data. Finally, we give the discussion and conclusion.

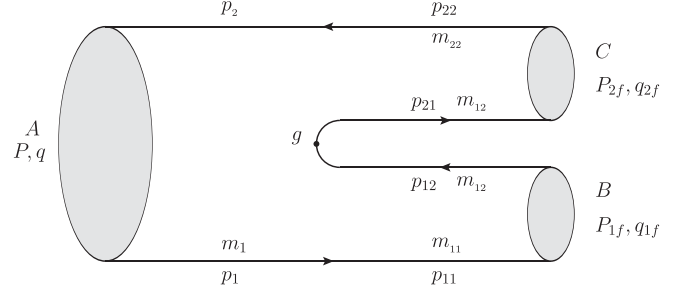


FIG. 1. The Feynman diagram for the two-body strong decay process with a 3P_0 vertex.

II. THE THEORETICAL CALCULATIONS

For the sake of brevity of the paper, the detailed introduction to the BS equation and 3P_0 model, as well as their combination, is not provided here. Interested readers may refer to [25–27,34,35] or our previous papers, for example, [47,49].

A. Transition amplitude of strong decay

The 3P_0 model [25] is nonrelativistic. Its core idea is that the quark and antiquark $q\bar{q}$ pair excited by the operator $g \int d\vec{x} \bar{\psi} \psi|_{\text{nonrel}}$ [50] from vacuum, carry vacuum quantum number, namely, $J^{PC} = 0^{++}$, which corresponds to a pair of quark and antiquark with $^{2L+1}L_J = ^3P_0$ quantum number, so it is called the 3P_0 model. In order to combine with the BS wave function, we extend this operator to the relativistic covariant form $-ig \int d^4x \bar{\psi} \psi$ (a similar form of interaction is also used in Refs. [31,51]), where g can be written as $2m_q\gamma$ and m_q is the constitute quark (u, d, s) mass. γ is the dimensionless interaction strength, and we take $\gamma = 0.4$ in this paper.

For the two-body strong decay $A \rightarrow B + C$, the Feynman diagram is shown in Fig. 1. Within the Mandelstam formalism [52], the transition amplitude of the strong decay $A \rightarrow B + C$ process can be written as

$$\begin{aligned} \langle P_{1f} P_{2f} | S | P \rangle_{^3P_0} &= (2\pi)^4 \delta^4(P - P_{1f} - P_{2f}) \mathcal{M}_{^3P_0} \\ &= -ig(2\pi)^4 \delta^4(P - P_{1f} - P_{2f}) \int \frac{d^4q}{(2\pi)^4} \text{Tr}[\chi_P(q) S_2^{-1}(-p_2) \bar{\chi}_{P_{2f}}(q_{2f}) \bar{\chi}_{P_{1f}}(q_{1f}) S_1^{-1}(p_1)], \end{aligned} \quad (1)$$

where $\chi_P(q)$, $\chi_{P_{1f}}(q_{1f})$, $\chi_{P_{2f}}(q_{2f})$ are the relativistic BS wave functions for initial and final mesons, respectively. The internal relative momenta of the initial and final mesons are q , q_{1f} , and q_{2f} , respectively. p_1 , p_2 , $S_1(p_1)$, and $S_2(-p_2)$ represent the momenta and propagators of the quark and antiquark, respectively.

Since we solve the complete Salpeter equation, not the BS equation, the instantaneous approximation has been used for the BS equation, and the Salpeter wave functions are obtained. So we make an instantaneous approximation to the upper amplitude, namely, integrate over the q_0 . Then we obtain the transition amplitude with the Salpeter wave functions as input [47,49],

$$\mathcal{M}_{^3P_0} = g \int \frac{d^3q_\perp}{(2\pi)^3} \text{Tr} \left[\frac{\not{P}}{M} \varphi_P^{++}(q_\perp) \frac{\not{P}}{M} \bar{\varphi}_{P_{2f}}^{++}(q_{2f\perp}) \bar{\varphi}_{P_{1f}}^{++}(q_{1f\perp}) \right] \left(1 - \frac{M - \omega_1 - \omega_2}{2\omega_{12}} \right), \quad (2)$$

where M is the mass of initial state, and φ_P^{++} and $\varphi_{P_{if}}^{++}$ are the positive energy wave functions of initial and final mesons, respectively. We have defined $q_\perp^\mu = q^\mu - (P \cdot q/M^2)P^\mu$. The relation between the relative momenta in initial and final mesons is $q_{if} = q + (-1)^{i+1}(\alpha_i P - \alpha_{ii} P_{if})$, where $i = 1, 2$, $\alpha_i = \frac{m_i}{m_1 + m_2}$, $\alpha_{ii} = \frac{m_{ii}}{m_{i1} + m_{i2}}$, and subscript f means this quantity belongs to the final state. $\omega_i = \sqrt{m_i^2 - q_\perp^2}$ and $\omega_{12} \equiv \sqrt{m_{12}^2 - p_{12\perp}^2}$. Considering $M \simeq \omega_1 + \omega_2$, the second term in parentheses can be ignored (when $|q_\perp|$ is large, this approximation is not true, but at this time, the value of the wave function is also very small, thus greatly reducing the contribution of this part).

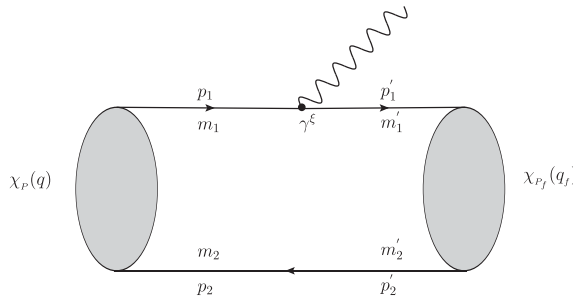
B. Transition amplitude of EM decay

For the EM decay of $A \rightarrow B\gamma$, the transition amplitude can be written as

$$\langle \chi_{cJ}(P_f, \epsilon_2) \gamma(k, \epsilon_0) | X(P, \epsilon_1) \rangle = (2\pi)^4 \delta^4(P - P_f - k) \epsilon_{0\xi} \mathcal{M}^\xi, \quad (3)$$

where ϵ_0 , ϵ_1 , and ϵ_2 are the polarization vectors (tensor) of the photon and initial and final mesons, respectively. P , P_f , and k are the momenta of the initial meson, final meson, and photon, respectively. From the quantum number perspective, we know that the electromagnetic processes of $^3D_3 \rightarrow ^3P_J \gamma$ ($J = 0, 1, 2$) are all E_1 dominant decays. But in nonrelativistic limit [16,53], the E_1 decay widths of $X(3842)$ to $\chi_{c0}\gamma$ and $\chi_{c1}\gamma$ are zero, so they are actually the M_2 dominant decays [54] and have very small partial widths. In addition, the channels $X(3842) \rightarrow \eta_c \gamma$ and $X(3842) \rightarrow c\bar{c}(^1D_2)\gamma$ are M_1 dominant modes and will not have large partial widths. Therefore, in this paper, we only calculate the E_1 dominant channel $X(3842) \rightarrow \chi_{c2}\gamma$ and ignore other electromagnetic modes.

From Fig. 2, we can see that invariant amplitude \mathcal{M}^ξ consists of two parts, where photons are emitted from the quark and antiquark, respectively. In the condition of instantaneous approach, the amplitude can be written as [42]



$$\mathcal{M}^\xi = \int \frac{d^3 q_\perp}{(2\pi)^3} \text{Tr} \left[Q_1 e \frac{\not{P}}{M} \bar{\varphi}_f^{++}(q_\perp + \alpha_2 P_{f\perp}) \gamma^\xi \varphi_i^{++}(q_\perp) + Q_2 e \bar{\varphi}_f^{++}(q_\perp - \alpha_1 P_{f\perp}) \frac{\not{P}}{M} \varphi_i^{++}(q_\perp) \gamma^\xi \right], \quad (4)$$

where Q_1 and Q_2 are the electric charges (in unit of e) of the quark and antiquark, respectively. $\varphi_{i,f}^{++}$ is the positive energy wave function, and i, f stand for initial and final states, respectively.

C. The relativistic wave functions

In the calculation, we use the relativistic Salpeter wave function for $X(3842)$, which is a 3^{--} state [55],

$$\varphi_{3^{--}}(q_\perp) = \epsilon_{\mu\nu\alpha} q_\perp^\mu q_\perp^\nu \left[q_\perp^\alpha \left(f_1 + \frac{\not{P}}{M} f_2 + \frac{\not{q}_\perp}{M} f_3 + \frac{\not{P}\not{q}_\perp}{M^2} f_4 \right) + M \gamma^\alpha \left(f_5 + \frac{\not{P}}{M} f_6 + \frac{\not{q}_\perp}{M} f_7 + \frac{\not{P}\not{q}_\perp}{M^2} f_8 \right) \right], \quad (5)$$

where $\epsilon_{\mu\nu\alpha}$ is the third-order polarization tensor of the state $X(3842)$. Radial wave function f_i ($i = 1, 2, \dots, 8$) is a function of $-q_\perp^2$, and its numerical value will be obtained by solving the Salpeter equation. In our method, not all radial wave functions f_i s are independent; only four of them are. The relationships between them are given in the Appendix.

We now show that every term in 3^{--} state wave function has negative parity and negative charge conjugate parity. When we perform parity transformation, $P' = (P_0, -\vec{P})$, $q' = (q_0, -\vec{q})$, and set

$$\varphi_{3^{--}}(P, q_\perp) = \eta_P \gamma_0 \varphi'_{3^{--}}(P', q'_\perp) \gamma_0,$$

where η_P is the parity. In the center of mass system, we have $P' = P$, $q'_\perp = -q_\perp$, and

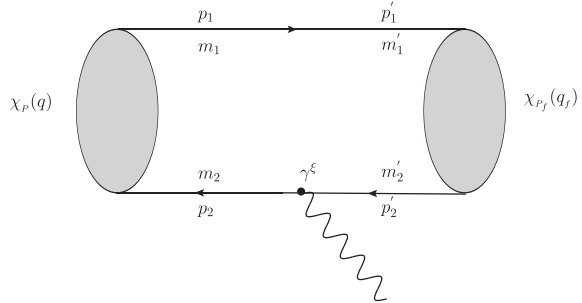


FIG. 2. Feynman diagram for the transition $\chi_P \rightarrow \chi_{cJ}\gamma$. The diagrams on the left and right show that photons come from the quark and the antiquark, respectively.

$$\begin{aligned}
\gamma_0 \phi'_{3--}(q'_\perp) \gamma_0 &= \epsilon_{\mu\nu\alpha} q_\perp^\mu q_\perp^\nu \left[-q_\perp^\alpha \gamma_0 \left(f_1 + \frac{\mathbf{P}}{M} f_2 - \frac{\mathbf{q}_\perp}{M} f_3 - \frac{\mathbf{P} \mathbf{q}_\perp}{M^2} f_4 \right) \gamma_0 \right. \\
&\quad \left. + M \gamma_0 \gamma^\alpha \left(f_5 + \frac{\mathbf{P}}{M} f_6 - \frac{\mathbf{q}_\perp}{M} f_7 - \frac{\mathbf{P} \mathbf{q}_\perp}{M^2} f_8 \right) \gamma_0 \right] \\
&= -\phi_{3--}(P, q_\perp),
\end{aligned} \tag{6}$$

so $\eta_P = -1$.

When we take the charge conjugate transformation,

$$\phi_{3--}(q_\perp) = \eta_C C \phi_{3--}^T(-q_\perp) C^{-1},$$

where T is the rotation transform, C is the charge conjugate transform, and $C \gamma_\mu^T C^{-1} = -\gamma_\mu$, η_C is the charge conjugate parity. We have

$$\begin{aligned}
C \phi_{3--}^T(-q_\perp) C^{-1} &= C \left\{ \epsilon_{\mu\nu\alpha} q_\perp^\mu q_\perp^\nu \left[-q_\perp^\alpha \left(f_1 + \frac{\mathbf{P}^T}{M} f_2 - \frac{\mathbf{q}_\perp^T}{M} f_3 - \frac{\mathbf{q}_\perp^T \mathbf{P}^T}{M^2} f_4 \right) \right. \right. \\
&\quad \left. \left. + M \left(f_5 + \frac{\mathbf{P}^T}{M} f_6 - \frac{\mathbf{q}_\perp^T}{M} f_7 - \frac{\mathbf{q}_\perp^T \mathbf{P}^T}{M^2} f_8 \right) \gamma^{\alpha T} \right] \right\} C^{-1} \\
&= -\epsilon_{\mu\nu\alpha} q_\perp^\mu q_\perp^\nu \left[q_\perp^\alpha \left((f_1 + 2f_7) + \frac{\mathbf{P}}{M} (2f_8 - f_2) + \frac{\mathbf{q}_\perp}{M} f_3 + \frac{\mathbf{P} \mathbf{q}_\perp}{M^2} f_4 \right) \right. \\
&\quad \left. + M \gamma^\alpha \left(f_5 + \frac{\mathbf{P}}{M} f_6 - \frac{\mathbf{q}_\perp}{M} f_7 + \frac{\mathbf{P} \mathbf{q}_\perp}{M^2} f_8 \right) \right] \\
&= -\phi_{3--}(q_\perp),
\end{aligned} \tag{7}$$

so $\eta_C = -1$. Since only quarkonium has C parity, we have used $m_1 = m_2$, $\omega_1 = \omega_2$, $f_2 = f_8$, and $f_7 = 0$ in Eq. (7), see the Appendix.

Further, we show that the relativistic wave function in Eq. (5) for the 3^{--} state is not a pure D wave. In terms of spherical harmonics Y_{lm} , we can rewrite

$$\epsilon_{\mu\nu\alpha} q_\perp^\mu q_\perp^\nu q_\perp^\alpha = 2i \sqrt{\frac{6\pi}{35}} |\vec{q}|^3 (Y_{32} - Y_{3-2}), \tag{8}$$

so f_1 and f_2 terms are F wave. Similarly, for the f_3 and f_4 terms,

$$\begin{aligned}
\epsilon_{\mu\nu\alpha} q_\perp^\mu q_\perp^\nu q_\perp^\alpha \mathbf{q}_\perp &= i |\vec{q}|^4 \left[\frac{4}{7} \sqrt{\frac{3\pi}{5}} (-Y_{21} \gamma^+ + Y_{2-1} \gamma^-) + \frac{2}{7} \sqrt{\frac{6\pi}{5}} (-Y_{22} + Y_{2-2}) \gamma^\Delta \right. \\
&\quad \left. + \frac{2}{7} \sqrt{\frac{2\pi}{5}} (Y_{41} \gamma^+ - Y_{4-1} \gamma^-) + \frac{4}{7} \sqrt{\frac{2\pi}{5}} (-Y_{42} + Y_{4-2}) \gamma^\Delta + 2 \sqrt{\frac{2\pi}{35}} (Y_{43} \gamma^- - Y_{4-3} \gamma^+) \right],
\end{aligned} \tag{9}$$

where $\gamma^+ = -\frac{\gamma^1 + i\gamma^2}{\sqrt{2}}$, $\gamma^- = \frac{\gamma^1 - i\gamma^2}{\sqrt{2}}$ and $\gamma^\Delta = \gamma^3$. So f_3 and f_4 terms include D wave and G wave, so they are $D - G$ mixing. The pure G wave in Eq. (5) is

$$\epsilon_{\mu\nu\alpha} q_\perp^\mu q_\perp^\nu q_\perp^\alpha \left(\frac{\mathbf{q}_\perp}{M} f_3 + \frac{\mathbf{P} \mathbf{q}_\perp}{M^2} f_4 \right) + \frac{3}{7} \epsilon_{\mu\nu\alpha} q_\perp^\mu q_\perp^\nu M \gamma^\alpha \frac{|\vec{q}|^2}{M^2} \left(f_3 - \frac{\mathbf{P}}{M} f_4 \right).$$

The f_5 and f_6 terms are D wave, because

$$\epsilon_{\mu\nu\alpha} q_\perp^\mu q_\perp^\nu q_\perp^\alpha = 2i \sqrt{\frac{2\pi}{15}} |\vec{q}|^2 [\sqrt{2} (Y_{21} \gamma^+ - Y_{2-1} \gamma^-) + (Y_{22} - Y_{2-2}) \gamma^\Delta]. \tag{10}$$

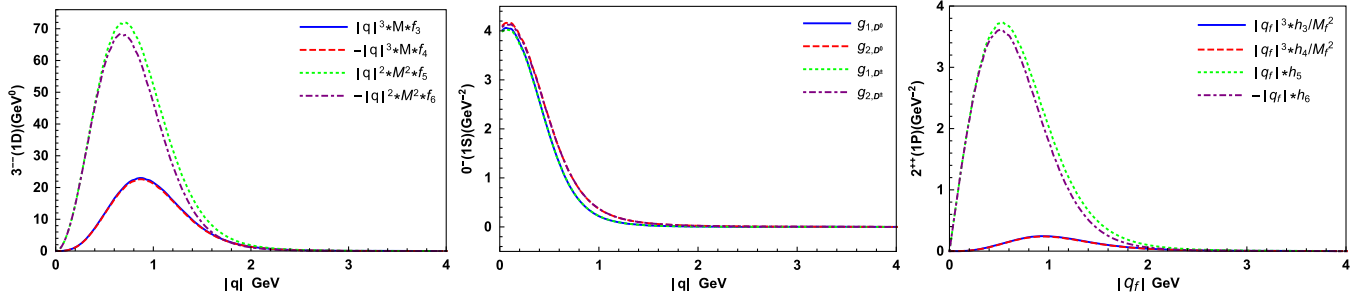


FIG. 3. The radial wave functions of the 3^{--} state $X(3842)$, 0^- states D^+ (D^-) and D^0 (\bar{D}^0), and 2^{++} state χ_{c2} , from left to right, respectively.

Then the complete D wave in Eq. (5) is

$$\epsilon_{\mu\nu\alpha} q_{\perp}^{\mu} q_{\perp}^{\nu} M \gamma^{\alpha} \left(f_5 + \frac{\not{p}}{M} f_6 \right) - \frac{3}{7} \epsilon_{\mu\nu\alpha} q_{\perp}^{\mu} q_{\perp}^{\nu} M \gamma^{\alpha} \frac{|\vec{q}|^2}{M^2} \left(f_3 - \frac{\not{p}}{M} f_4 \right).$$

The f_7 and f_8 terms are F wave, since

$$\begin{aligned} \epsilon_{\mu\nu\alpha} q_{\perp}^{\mu} q_{\perp}^{\nu} \gamma_{\perp}^{\alpha} \not{q}_{\perp} &= 2i|\vec{q}|^3 \left[\frac{2}{5} \sqrt{\frac{\pi}{7}} Y_{30}(\gamma^{+2} - \gamma^{-2}) \right. \\ &+ \frac{1}{5} \sqrt{\frac{6\pi}{7}} (-Y_{31}\gamma^{+} + Y_{3-1}\gamma^{-}) \gamma^{\Delta} \\ &+ \sqrt{\frac{2\pi}{105}} (Y_{32} - Y_{3-2})(2\gamma^{+}\gamma^{-} - \gamma^{\Delta^2}) \\ &\left. + \sqrt{\frac{2\pi}{35}} (Y_{33}\gamma^{-} - Y_{3-3}\gamma^{+}) \gamma^{\Delta} \right]. \end{aligned} \quad (11)$$

So, it can be concluded from our relativistic wave function that the widely used representations of $P = (-1)^{L+1}$ and $C = (-1)^{L+S}$, as well as $^{2S+1}L_J$, can only be strictly used in a nonrelativistic condition.

For strong decay final states, they can only be 0^- state pseudoscalars D^0 and \bar{D}^0 (or D^+ and D^-). The relativistic wave function of a 0^- state can be written as [36]

$$\varphi_{0-}(q_{f\perp}) = M_f \left(\frac{\not{p}_f}{M_f} g_1 + g_2 + \frac{\not{q}_{f\perp}}{M_f} g_3 + \frac{\not{p}_f \not{q}_{f\perp}}{M_f^2} g_4 \right) \gamma^5, \quad (12)$$

where the subscript f indicates that the quantity is in the final state. The radial wave functions g_3 and g_4 are not independent, they are related to g_1 and g_2 . We show their relationship in the Appendix. Similarly, the relativistic 0^- state wave function is not a pure S wave (the terms including g_1 and g_2), but also contains a small component of P wave (terms including g_3 and g_4).

The final state of EM decay is the charmonium 2^{++} state χ_{c2} , and its relativistic wave function can be written as [39]

$$\begin{aligned} \varphi_{2^{++}}(q_{f\perp}) &= \epsilon_{\mu\nu} q_{f\perp}^{\mu} \left[q_{f\perp}^{\nu} \left(h_1 + \frac{\not{p}_f}{M_f} h_2 + \frac{\not{q}_{f\perp}}{M_f} h_3 + \frac{\not{p}_f \not{q}_{f\perp}}{M_f^2} h_4 \right) \right. \\ &+ M_f \gamma^{\nu} \left(h_5 + \frac{\not{p}_f}{M_f} h_6 + \frac{\not{q}_{f\perp}}{M_f} h_7 \right) \\ &\left. + \frac{i}{M_f} h_8 \epsilon^{\mu\alpha\beta\gamma} P_{f\alpha} q_{f\perp\beta} \gamma_{\gamma} \gamma_5 \right], \end{aligned} \quad (13)$$

where $\epsilon_{\mu\nu}$ is the second-order polarization tensor, and $\epsilon_{\mu\nu\alpha\beta}$ is the Levi-Civita symbol. Four radial wave functions h_3 , h_4 , h_5 , and h_6 are independent, others are related to them; see the Appendix. The wave function of the 2^{++} state is P wave dominant, but also contains other partial waves. In Eq. (13), the terms including h_5 and h_6 are P waves, those including h_3 and h_4 are $P-F$ mixing waves, others are D waves.

We do not show the details of solving the complete Salpeter equations and only give the numerical values of independent radial wave functions in Fig. 3. From Fig. 3, we can see that $f_5 \simeq -f_6$, $g_1 \simeq g_2$, and $h_5 \simeq -h_6$. These equality relations under the nonrelativistic condition confirm the correctness of our method.

D. The form factors

Inserting Eqs. (5) and (12) into Eq. (2), where we integrate internal momentum q_{\perp} over the initial and final state wave functions, and finishing the trace, then we obtain the strong decay amplitude described using the form factor,

$$\mathcal{M}(X(3842) \rightarrow D\bar{D}) = \epsilon_{\mu\nu\alpha} P_f^{\mu} P_f^{\nu} P_f^{\alpha} t_1, \quad (14)$$

where t_1 is the form factor.

In the same way, inserting Eqs. (5) and (13) into Eq. (4), the EM transition amplitude described by the form factors is obtained as

$$\begin{aligned} \mathcal{M}^\xi(X(3842) \rightarrow \chi_{c2}(1P)\gamma) = & P^\xi \epsilon_{P_f P_f P_f} \epsilon_{f,PP} s_1 + P^\xi \epsilon_{\rho P_f P_f} \epsilon_{f,P}^\rho s_2 + \epsilon_{P_f P_f}^\xi \epsilon_{f,PP} s_3 + \epsilon_{P_f P_f} \epsilon_{f,P}^\xi s_4 \\ & + P^\xi \epsilon_{\rho\sigma P_f} \epsilon_{f,P}^{\rho\sigma} s_5 + \epsilon_{\rho P_f}^\xi \epsilon_{f,P}^\rho s_6 + \epsilon_{\rho P_f P_f} \epsilon_{f,P}^{\rho\sigma} s_7 + \epsilon_{\rho\sigma}^\xi \epsilon_{f,P}^{\rho\sigma} s_8, \end{aligned} \quad (15)$$

where s_i is the form factor. We have used some abbreviations, for example, $\epsilon_{P_f P_f P_f} \epsilon_{f,PP} = \epsilon_{\mu\nu\alpha} P_f^\mu P_f^\nu P_f^\alpha \epsilon_{f,\beta\gamma} P^\beta P^\gamma$. Since the expressions of t_1 and s_i are complex, the details are not shown here.

For the EM decay, we note that not all the form factors are independent, due to the Ward identity $(P_\xi - P_{f,\xi})\mathcal{M}^\xi = 0$, we have the following relations

$$\begin{aligned} s_3 &= (M^2 - ME_f)s_1 + s_4, & s_6 &= (M^2 - ME_f)s_2 + s_7, \\ s_8 &= (M^2 - ME_f)s_5. \end{aligned} \quad (16)$$

The two-body decay width formulation is

$$\Gamma(X \rightarrow AB) = \frac{|\vec{P}_f|}{8\pi M^2} \frac{1}{2J+1} \sum_\lambda |\overline{\mathcal{M}}|^2, \quad (17)$$

where $|\vec{P}_f| = \sqrt{[M^2 - (M_{1f} - M_{2f})^2][M^2 - (M_{1f} + M_{2f})^2]} / 2M$ is the three-dimensional momentum of the final meson, $J = 3$ is the total angular momentum of the initial meson, and λ represents the polarization of both initial and final mesons.

III. RESULTS AND DISCUSSIONS

In our model, the following constituent quark masses are used, $m_u = 0.305$, $m_d = 0.311$, $m_c = 1.62$ GeV. Other model dependent parameters can be found in Ref. [40], where we choose the Cornell potential [3], a linear scalar potential plus a Coulomb vector potential, since the predicted mass spectrum may not match very well with the experiment data, and a free constant parameter V_0 is usually added to the linear scalar potential to fit data [4]. So by varying the V_0 [40], we fit the experimental meson masses $M_{X(3842)} = 3.8427$, $M_{D^+} = 1.8697$, $M_{D^0} = 1.8648$, $M_{\chi_{c2}} = 3.5562$ GeV [5] and obtain the numerical values of the corresponding wave functions.

A. Strong decay widths of $X(3842)$ as the 1^3D_3 state

The strong decay widths of $X(3842)$ decays to $D^0\bar{D}^0$ and D^+D^- are calculated as

$$\begin{aligned} \Gamma[X(3842) \rightarrow D^0\bar{D}^0] &= 1.27 \text{ MeV}, \\ \Gamma[X(3842) \rightarrow D^+D^-] &= 1.08 \text{ MeV}. \end{aligned} \quad (18)$$

For comparison, we show our results and other model predictions [15–17,23,56] and experimental data [13] in Table I. Here we also present the choice of the mass of the initial state $X(3842)$ by the different working groups. Eichten *et al.* calculated the decay widths of $1^3D_3 \rightarrow DD$ though the refined Cornell coupled-channel model [15] and the Cornell coupled-channel model [56], respectively. Barnes *et al.* used the 3P_0 model [16,17] to estimate the strong decay width of $1^3D_3(3^{--})$. Reference [16] took the mass 3849 MeV of 1^3D_3 , which is obtained through the relativistic Godfrey-Isgur model (GI model). The mass 3872 MeV is also utilized in Ref. [16], because they consider $X(3872)$ as a candidate for 1^3D_3 . Reference [17] used mass 3806 MeV, which is obtained by the nonrelativistic method (NR model). Yu and Wang [23] studied 1^3D_3 strong decay with QCD sum rules and the 3P_0 model.

From Table I, one can see that our prediction of the strong decay width, 2.35 MeV, is close to the center value of the experiment, $2.79^{+0.86}_{-0.86}$ MeV, and is consistent well with the result of Ref. [16], 2.27 MeV, and we all used similar masses for 1^3D_3 . In Table I, the ratio between two strong decay channels $X(3842) \rightarrow D^+D^-$ and $X(3842) \rightarrow D^0\bar{D}^0$ is also shown. Our result

$$\frac{\mathcal{B}[X(3842) \rightarrow D^+D^-]}{\mathcal{B}[X(3842) \rightarrow D^0\bar{D}^0]} = 0.84 \quad (19)$$

is consistent well with others shown in Table I. The reason for the good agreement between different theoretical results is simple, as the ratio between the decay width of

TABLE I. The strong decay widths (MeV) of the $X(3842) \rightarrow DD$ and the ratio of $\frac{\mathcal{B}[X(3842) \rightarrow D^+D^-]}{\mathcal{B}[X(3842) \rightarrow D^0\bar{D}^0]}$.

	[15]	[16]	[17]	[23]	[56]	Ours	EX [13]
$M_{(1^3D_3)}$ (MeV)	3868	3849 3872	3806	3762–3912	3872 3902	3842.7	3842.71 $^{+0.28}_{-0.28}$
$\Gamma(X(3842) \rightarrow D^+D^-)$				2–3	0.39 0.72	1.08	
$\Gamma(X(3842) \rightarrow D^0\bar{D}^0)$				2.5–3.5	0.47 0.84	1.27	
$\Gamma(X(3842) \rightarrow DD)$	0.82	2.27 4.04	0.5	4.5–6.5	0.86 1.56	2.35	2.79 $^{+0.86}_{-0.86}$
$\frac{\Gamma(X(3842) \rightarrow D^+D^-)}{\Gamma(X(3842) \rightarrow D^0\bar{D}^0)}$				0.85–0.90	0.83 0.86	0.84	

TABLE II. The radiative partial decay widths (keV) of the $X_{(1^3D_3)}(3842) \rightarrow \chi_{c2}\gamma$.

Model	[17]		[22]				[56]				
	NR	GI	NR	V	S	RE	SC^3		C^3		
$M_{(1^3D_3)}$ (MeV)	3806	3849			3815		3815	3868	3972	3815	3868
$\Gamma(X(3842) \rightarrow \chi_{c2}\gamma)$	272	296	252	163	170	156	199	329	341	179	286
Model	[57]		[58]			[59]		[60]		Ours	
	NR	SN_0	SN_1	NR	MNR	CCP_v		NR	RE	BS	
$M_{(1^3D_3)}$ (MeV)		3799		3815	3813	3520	3653	3831	3805	3842.7	
$\Gamma(X(3842) \rightarrow \chi_{c2}\gamma)$	272	284	223	340	302	138	246	432	271	298	288

$X(3842) \rightarrow D^+D^-$ and those of $X(3842) \rightarrow D^0\bar{D}^0$ is mainly determined by the phase spaces. In Eq. (14), the decay amplitude of $X(3842) \rightarrow D\bar{D}$ is written as $\mathcal{M} = \epsilon_{\mu\nu\alpha} P_f^\mu P_f^\nu P_f^\alpha t_1$, so

$$\sum_{\lambda} |\overline{\mathcal{M}}|^2 = \frac{2}{5} |\vec{P}_f|^6 t_1^2,$$

the form factor t_1 is an overlapping integral of initial and final radial wave functions, and from Fig. 3, it can be seen that there is not much difference in the radial wave functions between D^+ and D^0 mesons. Then using Eq. (17) of the decay width, we obtain

$$\frac{\Gamma(X(3842) \rightarrow D^+D^-)}{\Gamma(X(3842) \rightarrow D^0\bar{D}^0)} \propto \frac{(|\vec{P}_f|_{D^+})^7}{(|\vec{P}_f|_{D^0})^7} = 0.735. \quad (20)$$

This estimation is very close to our calculated value 0.84, indicating that the difference between the decay widths of $X(3842) \rightarrow D^0\bar{D}^0$ and $X(3842) \rightarrow D^+D^-$ is almost purely from the phase space difference, and the isospin symmetry breaking effect is small.

Since the very small mass difference ($2M_{D^+} - 2M_{D^0}$) causes a large difference in partial decay widths, and the 1^3D_3 state $X(3842)$ just lies above the threshold of two charmed mesons, we draw a conclusion that the mass of $X(3842)$ has a significant impact on the value of its strong decay widths. Therefore, accurate experimental mass measurements are crucial for theoretical study on strong decays.

B. EM decay width of $X(3842)$ as the 1^3D_3 state

According to Refs. [17,53], only $\psi_3(1^3D_3) \rightarrow \chi_{c2}(1P)\gamma$ is dominant in the EM decays of $\psi_3(1^3D_3)$. Therefore, we only calculate the decay width of this channel, and the result is

$$\Gamma[X(3842) \rightarrow \chi_{c2}(1P)\gamma] = 288 \text{ keV}. \quad (21)$$

We show this result and other model predictions [17,22,56–60] in Table II for comparison, where the label NR represents the nonrelativistic potential model, the relativistic potential model is labeled RE; V and S denote the relativistic with vector and scalar potential model; C^3 and SC^3 are Cornell coupled-channel model and single channel potential model; SN_0 (with the zeroth-order wave functions) and SN_1 (with first-order relativistically corrected wave functions) signify the screened nonrelativistic potential model; CCP_v represents Coulomb plus power form of the interquark potential with exponent v . As can be seen from Table II, different models led to different results. Most of these results are distributed between 150–350 keV. Our result, 288 keV, is in good agreement with the 296 keV of the GI model [17], the 286 keV of the C^3 model [56], and the 298 keV of the relativistic model [60].

In a previous paper [41], we pointed out that, in the complete relativistic method, the relativistic wave function of a state is not a pure wave. This conclusion is also valid for the charmonium [54]. For the $X(3842)$ as the 3^{--} state $\psi_3(1^3D_3)$, the D partial wave that survives in the non-relativistic limit is dominant, while the F and G partial waves that are the relativistic correction are small. Similarly,

TABLE III. The EM decay width (keV) of different partial waves for $X_{(1^3D_3)}(3842) \rightarrow \chi_{c2}(1P)\gamma$.

3^{--}	2^{++}			
	Complete	P wave (D_{f_5}, D_{f_6})	D wave ($D_{f_1}, D_{f_2}, D_{f_7}$)	F wave (D_{f_3}, D_{f_4})
Complete	288	215	18.2	0.197
D wave (F_5, F_6)	234	232	13.9	0.186
F wave (F_1, F_2, F_7)	13.7	13.4	0.180	0.0187
G wave (F_3, F_4)	0.540	0.245	0.00373	0.000358

for the $\chi_{c2}(1P)$, as the 2^{++} state, beside the main non-relativistic P wave, it also contain a small part of relativistic D and F partial waves. To see these clearly, we study the contribution of different partial waves in the decay $\psi_3(1^3D_3) \rightarrow \chi_{c2}(1P)\gamma$. The results are presented in Table III, where “complete” means the complete or whole wave function is used, “D wave” means only the D partial wave has contribution and other partial waves are deleted.

From Table III, we can see that, for the initial state, compared to F and G waves, the D wave has the dominant contribution. The main contribution of the final state comes from the P wave, which provides the nonrelativistic result, and the relativistic correction (D and F waves in 2^{++} state) contribution is relatively small. Using the nonrelativistic result, 232 keV, and the relativistic one, 288 keV, we obtain the relativistic effect is 19%.

IV. DISCUSSION AND CONCLUSION

In a previous paper [55], we have estimated the annihilation decay (including ggg and $gg\gamma$ final states) width of $X(3842)$, which is about 26.5 keV. From the work of Barnes and Godfrey [16], we get the partial decay width $\Gamma[\psi_3(^3D_3) \rightarrow J/\psi\pi\pi] \approx 210$ keV, which is a dominant $E_1 - E_1$ multipole hadronic transition, and ignore other multipole transitions that have smaller contributions compared with the $E_1 - E_1$ transition, like the $M_1 - M_1$ and $E_1 - M_2$ mode $X(3842) \rightarrow J/\psi\eta$, etc. Then the total decay width of $X(3842)$ can be estimated as

$$\begin{aligned} \Gamma[X(3842)] &\approx \Gamma(DD) + \Gamma(\chi_{c2}\gamma) + \Gamma(J/\psi\pi\pi) \\ &+ \Gamma(ggg) + \Gamma(gg\gamma) = 2.87 \text{ MeV}. \end{aligned} \quad (22)$$

This result is in good agreement with the experimental data $2.79^{+0.86}_{-0.86}$ MeV.

In conclusion, we study the strong and EM decays of $X(3842)$ as the $\psi_3(1^3D_3)$ state by using the relativistic Bethe-Salpeter method and the 3P_0 model. Our results are $\Gamma[X(3842) \rightarrow D^0\bar{D}^0] = 1.27$ MeV, $\Gamma[X(3823) \rightarrow D^+D^-] = 1.08$ MeV, $\Gamma[X(3842) \rightarrow \chi_{c2}(1P)\gamma] = 288$ keV, and the ratio $\frac{B[X(3842) \rightarrow D^+D^-]}{B[X(3842) \rightarrow D^0\bar{D}^0]} = 0.84$. Compared with strong decay, the EM decay is not small, which is expected to be detected by experiment. In addition, we calculated the contributions of partial waves for $X(3842) \rightarrow \chi_{c2}(1P)\gamma$ and obtained the relativistic effect 19%. These results may provide useful information for $X(3842)$ as the charmonium $\psi_3(^3D_3)$.

ACKNOWLEDGMENTS

This work was supported in part by the National Natural Science Foundation of China (NSFC) under Grants No. 12075073, No. 12375085, No. 11865001, and No. 12075074, the Natural Science Foundation of Hebei province under the Grant No. A2021201009, and the Postgraduate's Innovation Fund Project of Hebei University under the Grant No. HBU2022BS002.

APPENDIX

1. Constrained conditions of radial wave function

For the 3^{--} state, we have the following relations between radial wave functions [55]:

$$\begin{aligned} f_1 &= \frac{q_{\perp}^2 f_3(\omega_1 + \omega_2) + 2M^2 f_5 \omega_2}{M(m_1 \omega_2 + m_2 \omega_1)}, & f_2 &= \frac{q_{\perp}^2 f_4(\omega_1 - \omega_2) + 2M^2 f_6 \omega_2}{M(m_1 \omega_2 + m_2 \omega_1)}, \\ f_7 &= \frac{M(\omega_1 - \omega_2)}{m_1 \omega_2 + m_2 \omega_1} f_5, & f_8 &= \frac{M(\omega_1 + \omega_2)}{m_1 \omega_2 + m_2 \omega_1} f_6. \end{aligned} \quad (A1)$$

For the 0^- state, we have [36]

$$g_3 = \frac{g_2 M_f(\omega_{2f} - \omega_{1f})}{(m_{1f} \omega_{2f} + m_{2f} \omega_{1f})}, \quad g_4 = -\frac{g_1 M_f(\omega_{2f} + \omega_{1f})}{(m_{1f} \omega_{2f} + m_{2f} \omega_{1f})}. \quad (A2)$$

For the 2^{++} state, the relations are [39]

$$\begin{aligned} h_1 &= \frac{(q_{f\perp}^2 h_3 + M_f^2 h_5)(\omega_{1f} + \omega_{2f}) - M_f^2 h_5(\omega_{1f} - \omega_{2f})}{M_f(m_{1f} \omega_{2f} + m_{2f} \omega_{1f})}, & h_2 &= \frac{(q_{f\perp}^2 h_4 - M_f^2 h_6)(\omega_{1f} - \omega_{2f})}{M_f(m_{1f} \omega_{2f} + m_{2f} \omega_{1f})}, \\ h_7 &= \frac{M_f(\omega_{1f} - \omega_{2f})}{m_{1f} \omega_{2f} + m_{2f} \omega_{1f}} h_5, & h_8 &= \frac{M_f(\omega_{1f} + \omega_{2f})}{m_{1f} \omega_{2f} + m_{2f} \omega_{1f}} h_6. \end{aligned} \quad (A3)$$

2. The positive energy wave functions

The positive energy wave function for the 3^{--} state is [55]

$$\varphi_{3^{--}}^{++}(q_{\perp}) = \epsilon_{\mu\nu\alpha} q_{\perp}^{\mu} q_{\perp}^{\nu} q_{\perp}^{\alpha} \left[F_1 + \frac{\not{p}}{M} F_2 + \frac{\not{q}_{\perp}}{M} F_3 + \frac{\not{p}\not{q}_{\perp}}{M^2} F_4 \right] + M \epsilon_{\mu\nu\alpha} \gamma^{\mu} q_{\perp}^{\nu} q_{\perp}^{\alpha} \left[F_5 + \frac{\not{p}}{M} F_6 + \frac{\not{p}\not{q}_{\perp}}{M^2} F_7 \right], \quad (\text{A4})$$

where

$$\begin{aligned} F_1 &= \frac{1}{2Mm_1\omega_1} [q_{\perp}^2(\omega_1 f_3 + m_1 f_4) + M^2(\omega_1 f_5 - m_1 f_6)], \\ F_2 &= \frac{M(-\omega_1 f_5 + m_1 f_6)}{m_1\omega_1}, \quad F_3 = \frac{1}{2} \left(f_3 + \frac{m_1}{\omega_1} f_4 - \frac{M^2}{m_1\omega_1} f_6 \right), \\ F_4 &= \frac{1}{2} \left(\frac{\omega_1}{m_1} f_3 + f_4 - \frac{M^2}{m_1\omega_1} f_5 \right), \quad F_5 = \frac{1}{2} \left(f_5 - \frac{\omega_1}{m_1} f_6 \right), \\ F_6 &= \frac{1}{2} \left(-\frac{m_1}{\omega_1} f_5 + f_6 \right), \quad F_7 = \frac{M}{2\omega_1} \left(-f_5 + \frac{\omega_1}{m_1} f_6 \right). \end{aligned}$$

The positive energy wave function of the 0^{-} state is [36]

$$\varphi_{0^{-}}^{++}(q_{f\perp}) = \left[G_{f_1} + \frac{\not{p}_{f\perp}}{M_f} G_{f_2} + \frac{\not{p}_f \not{q}_{f\perp}}{M_f^2} G_{f_3} \right] \gamma^5, \quad (\text{A5})$$

where

$$G_{f_1} = \frac{M_f}{2} \left[\frac{\omega_f}{m_f} g_1 + g_2 \right], \quad G_{f_2} = \frac{M_f}{2} \left[g_1 + \frac{m_f}{\omega_f} g_2 \right], \quad G_{f_3} = -\frac{M_f}{\omega_f} G_{f_1}.$$

The positive energy wave function for the 2^{++} state χ_{c2} is [37]

$$\varphi_{2^{++}}^{++}(q_{f\perp}) = \epsilon_{f,\mu\nu} q_{f\perp}^{\mu} q_{f\perp}^{\nu} \left[H_{f_1} + \frac{\not{p}_f}{M_f} H_{f_2} + \frac{\not{q}_{f\perp}}{M_f} H_{f_3} + \frac{\not{p}_f \not{q}_{f\perp}}{M_f^2} H_{f_4} \right] + M_f \epsilon_{f,\mu\nu} \gamma^{\mu} q_{f\perp}^{\nu} \left[H_{f_5} + \frac{\not{p}_f}{M_f} H_{f_6} + \frac{\not{p}_f \not{q}_{f\perp}}{M_f^2} H_{f_7} \right], \quad (\text{A6})$$

where

$$\begin{aligned} H_{f_1} &= \frac{1}{2M_f m_f \omega_f} (\omega_f q_{f\perp}^2 h_3 + m_f q_{f\perp}^2 h_4 + M_f^2 \omega_f h_5 - M_f^2 m_f h_6), \\ H_{f_2} &= \frac{M_f}{2m_f \omega_f} (m_f h_5 - \omega_f h_6), \quad H_{f_3} = \frac{1}{2} \left(h_3 + \frac{m_f}{\omega_f} h_4 - \frac{M_f^2}{m_f \omega_f} h_6 \right), \\ H_{f_4} &= \frac{1}{2} \left(\frac{\omega_f}{m_f} h_3 + h_4 - \frac{M_f^2}{m_f \omega_f} h_5 \right), \quad H_{f_5} = \frac{1}{2} \left(h_5 - \frac{\omega_f}{m_f} h_6 \right), \\ H_{f_6} &= \frac{1}{2} \left(-\frac{m_f}{\omega_f} h_5 + h_6 \right), \quad H_{f_7} = \frac{M_f}{2\omega_f} \left(-h_5 + \frac{\omega_f}{m_f} h_6 \right). \end{aligned}$$

- [1] E598 Collaboration, Experimental observation of a heavy particle J , *Phys. Rev. Lett.* **33**, 1404 (1974).
- [2] SLAC-SP-017 Collaboration, Discovery of a narrow resonance in e^+e^- annihilation, *Phys. Rev. Lett.* **33**, 1406 (1974).
- [3] E. Eichten, K. Gottfried, T. Kinoshita, K. D. Lane, and T.-M. Yan, Charmonium: The model, *Phys. Rev. D* **17**, 3090 (1978); **21**, 313(E) (1980).
- [4] S. Godfrey and N. Isgur, Mesons in a relativized quark model with chromodynamics, *Phys. Rev. D* **32**, 189 (1985).
- [5] K. A. Olive *et al.* (Particle Data Group), Review of particle physics, *Prog. Theor. Exp. Phys.* **2022**, 083C01 (2022).
- [6] S. K. Choi *et al.* (Belle Collaboration), Observation of a narrow charmonium-like state in exclusive $B^\pm \rightarrow K^\pm \pi^+ \pi^- J/\psi$ decays, *Phys. Rev. Lett.* **91**, 262001 (2003).
- [7] S. Uehara *et al.* (Bell Collaboration), Observation of a χ'_{c2} candidate in $\gamma\gamma \rightarrow D\bar{D}$ production at Belle, *Phys. Rev. Lett.* **96**, 082003 (2006).
- [8] B. Aubert *et al.* (BABAR Collaboration), Observation of the $\chi_{c2}(2P)$ meson in the reaction $\gamma\gamma \rightarrow D\bar{D}$ at BABAR, *Phys. Rev. D* **81**, 092003 (2010).
- [9] K. Abe *et al.* (Bell Collaboration), Observation of a new charmonium-like state produced in association with a J/ψ in e^+e^- annihilation at $\sqrt{s} \approx 10.6$ GeV, *Phys. Rev. Lett.* **98**, 082001 (2007).
- [10] P. Pakhlov *et al.* (Bell Collaboration), Production of new charmonium-like states in $e^+e^- \rightarrow J/\psi D^{(*)}\bar{D}^{(*)}$ at $\sqrt{s} \approx 10.6$ GeV, *Phys. Rev. Lett.* **100**, 202001 (2008).
- [11] J. P. Lees *et al.* (BABAR Collaboration), Study of $X(3915) \rightarrow J/\psi \omega$ in two-photon collisions, *Phys. Rev. D* **86**, 072002 (2012).
- [12] K. Chilikin *et al.* (Belle Collaboration), Observation of an alternative $\chi_{c0}(2P)$ candidate in $e^+e^- \rightarrow J/\psi D\bar{D}$, *Phys. Rev. D* **95**, 112003 (2017).
- [13] R. Aaij *et al.* (LHCb Collaboration), Near-threshold $D\bar{D}$ spectroscopy and observation of a new charmonium state, *J. High Energy Phys.* **07** (2019) 035.
- [14] M. Ablikim *et al.* (BESIII Collaboration), Measurement of $e^+e^- \rightarrow \pi^+\pi^- D^+D^-$ cross sections at center-of-mass energies from 4.190 to 4.946 GeV, *Phys. Rev. D* **106**, 052012 (2022).
- [15] E. J. Eichten, K. Lane, and C. Quigg, New states above charm threshold, *Phys. Rev. D* **73**, 014014 (2006).
- [16] T. Barnes and S. Godfrey, Charmonium options for the $X(3872)$, *Phys. Rev. D* **69**, 054008 (2004).
- [17] T. Barnes, S. Godfrey, and E. S. Swanson, Higher charmonia, *Phys. Rev. D* **72**, 054026 (2005).
- [18] E. J. Eichten and F. Feinberg, Spin-dependent forces in quantum chromodynamics, *Phys. Rev. D* **23**, 2724 (1981).
- [19] S. N. Gupta, S. F. Radford, and W. W. Repko, Semirelativistic potential model for heavy quarkonia, *Phys. Rev. D* **34**, 201 (1986).
- [20] L. P. Fulcher, Perturbative QCD, a universal QCD scale, long-range spin-orbit potential, and the properties of heavy quarkonia, *Phys. Rev. D* **44**, 2079 (1991).
- [21] J. Zeng, J. W. Van Orden, and W. Roberts, Heavy mesons in a relativistic model, *Phys. Rev. D* **52**, 5229 (1995).
- [22] D. Ebert, R. N. Faustov, and V. O. Galkin, Properties of heavy quarkonia and B_c mesons in the relativistic quark model, *Phys. Rev. D* **67**, 014027 (2003).
- [23] G.-L. Yu and Z.-G. Wang, Analysis of the $X(3842)$ as a D -wave charmonium meson, *Int. J. Mod. Phys. A* **34**, 1950151 (2019).
- [24] S. Piemonte, S. Collins, M. Padmanath, D. Mohler, and S. Prelovsek, Charmonium resonances with $J^{PC} = 1^{--}$ and 3^{--} from $D\bar{D}$ scattering on the lattice, *Phys. Rev. D* **100**, 074505 (2019).
- [25] L. Micu, Decay rates of meson resonances in a quark model, *Nucl. Phys.* **B10**, 521 (1969).
- [26] A. Le Yaouanc, L. Oliver, O. P'ene, and J. C. Raynal, "Naive" quark-pair-creation model of strong-interaction vertices, *Phys. Rev. D* **8**, 2223 (1973).
- [27] A. Le Yaouanc, L. Oliver, O. P'ene, and J. C. Raynal, Naive quark-pair-creation model and baryon decays, *Phys. Rev. D* **9**, 1415 (1974).
- [28] R. Kokoski and N. Isgur, Meson decays by flux tube breaking, *Phys. Rev. D* **35**, 907 (1987).
- [29] E. Eichten, K. Gottfried, T. Kinoshita, K. D. Lane, and T.-M. Yan, Charmonium: Comparison with experiment, *Phys. Rev. D* **21**, 203 (1980).
- [30] E. S. Ackleh, T. Barnes, and E. S. Swanson, On the mechanism of open-flavor strong decays, *Phys. Rev. D* **54**, 6811 (1996).
- [31] Yu. A. Simonov, Di-pion decays of heavy quarkonium in the field correlator method, *Phys. At. Nucl.* **71**, 1048 (2008).
- [32] Z.-K. Geng, T. wang, Y. Jiang, G. Li, X.-Z. Tan, and G.-L. Wang, Relativistic effects in the semileptonic B_c decays to charmonium with the Bethe-Salpeter method, *Phys. Rev. D* **99**, 013006 (2019).
- [33] G.-L. Wang, T.-F. Feng, and X.-G. Wu, Average speed and its powers v^n of a heavy quark in quarkonia, *Phys. Rev. D* **101**, 116011 (2020).
- [34] E. E. Salpeter, Mass corrections to the fine structure of hydrogen-like atoms, *Phys. Rev.* **87**, 328 (1952).
- [35] E. E. Salpeter and H. A. Bethe, A relativistic equation for bound state problems, *Phys. Rev.* **84**, 1232 (1951).
- [36] C. S. Kim and G.-L. Wang, Average kinetic energy of heavy quark (μ_π^2) inside heavy meson in 0^- state by Bethe-Salpeter method, *Phys. Lett. B* **584**, 285 (2004).
- [37] G.-L. Wang, Decay constants of heavy vector mesons in relativistic Bethe-Salpeter method, *Phys. Lett. B* **633**, 492 (2006).
- [38] G.-L. Wang, Decay constants of P -wave mesons, *Phys. Lett. B* **650**, 15 (2007).
- [39] G.-L. Wang, Annihilation rate of 2^{++} charmonium and bottomonium, *Phys. Lett. B* **674**, 172 (2009).
- [40] C.-H. Chang and G.-L. Wang, Spectrum for heavy quarkonia and mixture of the relevant wave functions within the framework of Bethe-Salpeter equation, *Sci. China Phys. Mech. Astron.* **53**, 2005 (2010).
- [41] G.-L. Wang, T.-H. Wang, Q. Li, and C.-H. Chang, The mass spectrum and wave functions of the B_c system, *J. High Energy Phys.* **05** (2022) 006.
- [42] C.-H. Chang, J.-K. Chen, and G.-L. Wang, Instantaneous formulation for transitions between two instantaneous bound states and its gauge invariance, *Commun. Theor. Phys.* **46**, 467 (2006).
- [43] H.-F. Fu, G.-L. Wang, Z.-H. Wang, and X.-J. Chen, Semi-leptonic and non-leptonic B meson decays to charmed mesons, *Chin. Phys. Lett.* **28**, 121301 (2011).

- [44] Q. Li, Y. Jiang, T. Wang, H. Yuan, G.-L. Wang, and C.-H. Chang, Study of the excited 1^- charm and charm-strange mesons, *Eur. Phys. J. C* **77**, 297 (2017).
- [45] Z.-H. Wang and G.-L. Wang, Two-body strong decays of the 2P and 3P charmonium states, *Phys. Rev. D* **106**, 054037 (2022).
- [46] F. E. Close and E. S. Swanson, Dynamics and decay of heavy-light hadrons, *Phys. Rev. D* **72**, 094004 (2005).
- [47] T. Wang, G.-L. Wang, H.-F. Fu, and W.-L. Ju, Two-body strong decay of $Z(3930)$ as the $\chi_{c2}(2P)$ state, *J. High Energy Phys.* **07** (2013) 120.
- [48] S.-C. Li, T. Wang, Y. Jiang, X.-Z. Tan, Q. Li, G.-L. Wang, and C.-H. Chang, Strong decays of $D_J(3000)$ and $D_{sJ}(3040)$, *Phys. Rev. D* **97**, 054002 (2018).
- [49] H.-F. Fu, X.-J. Chen, G.-L. Wang, and T.-H. Wang, OZI-allowed two body Υ decays in the 3P_0 model with the relativistic wave functions, *Int. J. Mod. Phys. A* **27**, 1250027 (2012).
- [50] E. S. Swanson, The new heavy mesons: A status report, *Phys. Rep.* **429**, 243 (2006).
- [51] I. V. Danilkin and Yu. A. Simonov, Dynamical origin and the pole structure of $X(3872)$, *Phys. Rev. Lett.* **105**, 102002 (2010).
- [52] S. Mandelstam, Dynamical variables in the Bethe-Salpeter formalism, *Proc. R. Soc. A* **233**, 248 (1955).
- [53] W. Kwong and J. L. Rosner, D -wave quarkonium levels of the Υ family, *Phys. Rev. D* **38**, 279 (1988).
- [54] W. Li, S.-Y. Pei, T. Wang, Y.-L. Wang, T.-F. Feng, and G.-L. Wang, Electromagnetic decays of $X(3823)$ as the $\psi_2(1^3D_2)$ state and its radial excited states, *Phys. Rev. D* **107**, 113002 (2023).
- [55] T. Wang, H.-F. Fu, Y. Jiang, Q. Li, and G.-L. Wang, Annihilation rates of $^3D_2(2^{--})$ and $^3D_3(3^{--})$ heavy quarkonia, *Int. J. Mod. Phys. A* **32**, 1750035 (2017).
- [56] E. J. Eichten, K. Lane, and C. Quigg, Charmonium levels near threshold and the narrow state $X(3872) \rightarrow \pi^+\pi^-J/\psi$, *Phys. Rev. D* **69**, 094019 (2004).
- [57] B.-Q. Li and K.-T. Chao, Higher charmonia and X , Y , Z states with screened potential, *Phys. Rev. D* **79**, 094004 (2009).
- [58] L. Cao, Y.-C. Yang, and H. Chen, Charmonium states in QCD-inspired quark potential model using gaussian expansion method, *Few-Body Syst.* **53**, 327 (2012).
- [59] A. Parmar, B. Patel, and P. Vinodkumar, Two-photon, two-gluon and radiative decays of heavy flavoured mesons, *Nucl. Phys.* **A848**, 299 (2010).
- [60] M. A. Sultan, N. Akbar, B. Masud, and F. Akram, Higher hybrid charmonia in an extended potential model, *Phys. Rev. D* **90**, 054001 (2014).